A screen for regulators of survival of motor neuron protein levels

Published in final edited form as:
Nat Chem Biol. 2011 ; 7(8): 544–552. doi:10.1038/nchembio.595.

A Screen for Regulators of Survival of Motor Neuron Protein Levels

Nina R. Makhortova[1,2], **Monica Hayhurst**[1,2], **Antonio Cerqueira**[1,2], **Amy D. Sinor-Anderson**[1,4], **Wen-Ning Zhao**[1,5], **Patrick W. Heiser**[1,6], **Anthony C. Arvanites**[2], **Lance S. Davidow**[2], **Zachary O. Waldon**[3], **Judith A. Steen**[3], **Kelvin Lam**[2], **Hien D. Ngo**[2], and **Lee L. Rubin**[1,2,*]

[1]Department of Stem Cell and Regenerative Biology, Harvard University, 7 Divinity Avenue, Cambridge, MA 02138, USA

[2]Harvard Stem Cell Institute, Harvard University, 7 Divinity Avenue, Cambridge, MA 02138, USA

[3]Children's Hospital Boston, F.M. Kirby Neurobiology Center, 300 Longwood Ave, CLS12032, Boston, MA 02115

Abstract

The motor neuron disease Spinal Muscular Atrophy (SMA) results from mutations that lead to low levels of the ubiquitously expressed protein Survival of Motor Neuron (SMN). Ever-increasing data suggest that therapeutics that elevate SMN may be effective in treating SMA. We executed an image-based screen of annotated chemical libraries and discovered multiple classes of compounds that were able to increase cellular SMN. Among the most important was the RTK/PI3K/AKT/GSK-3 signaling cascade. Chemical inhibitors of GSK-3, as well as shRNAs directed against this target, elevate SMN levels primarily by stabilizing the protein. Of particular significance is that GSK-3 chemical inhibitors were also effective in motor neurons, not only in elevating SMN levels, but also in blocking the death that was produced when SMN was acutely reduced by a SMN-specific shRNA. Thus, we have established a screen capable of detecting drug-like compounds that correct the main phenotypic change that underlies SMA.

Keywords

Spinal muscular atrophy; small molecule screen; SMN; GSK-3; motor neuron

INTRODUCTION

The neuromuscular disorder Spinal Muscular Atrophy (SMA) is the most common genetic cause of death in young children. The disease is known to be associated with defects — deletions or particular mutations in the Survival of Motor Neuron 1 (*SMN1*) gene — that result in a severe reduction of SMN1 protein[1]. The *SMN1* gene has been duplicated in

*Correspondence should be addressed to L.L.R. (lee_rubin@harvard.edu).
[4]Current Address: Thermo Fisher Scientific, 100 Technology Drive, Pittsburgh PA 15219
[5]Current Address: Center for Human Genetic Research, Massachusetts General Hospital, 185 Cambridge Street, Boston, MA 02114
[6]Current Address: Ferring Pharmaceuticals Inc., 4 Gatehall Drive, Parsippany, NJ 07054

Author contributions.
NRM, MH, AC, ADS, WZ and PWH designed, carried out the experiments and analyzed results. HDN carried out experiments. ACA, LSD and KL analyzed screening results. ZOW and JAS performed Mass Spectrometry and analyzed results. LLR designed experiments and analyzed results. NRM, MH and LLR wrote the manuscript.

Declaration of competing financial interests: LLR is a founder of iPierian, Inc. and a member of its Scientific Advisory Board.

primates, and survival is determined by the level of expression of the duplicated gene (*SMN2*), which, because of a nucleotide substitution in exon 7, codes mostly for an unstable truncated protein and for a small percentage of completely active full-length protein[2,3]. Neuromuscular function and survival improve dramatically with increased number of copies of the *SMN2* gene which, consequently, elevate the level of full-length SMN[4]. In fact, one of the peculiarities of the disease relates to the relationship between cell survival and quantity of SMN. Since parental carriers of SMA are phenotypically normal, presumably only approximately 50% of wildtype SMN levels are required[5,6], but when the level of SMN is reduced sufficiently, probably greater than 80%, most or all cells die. For example, mice lacking Smn cannot reach the blastocyst stage[7]. Importantly, there seems to be a critical level at which many cell types are relatively unaffected, but a few cell types, such as motor neurons and possibly muscle cells, are compromised[8].

The motor neuron sensitivity to low levels of SMN in particular is not well understood given that it is a ubiquitously expressed protein. It is known that SMN is part of a complex that contains several other proteins, Gemins 2–7, and is found in all metazoan cells. SMN is localized in the cytoplasm and in nuclear structures called Gems that appear to be similar to and possibly interact with coiled bodies[9]. The full spectrum of SMN functions in nucleus and cytoplasm has not been determined, but the nuclear SMN is clearly thought to participate in pre-mRNA splicing[10]. The cytoplasmic SMN has also been claimed to be involved in splicing[11] but this is controversial[12,13]. Additionally, in neurons, cytoplasmic SMN may play a role in mRNA transport[14,15] and, possibly, in axon growth[16] and ion channel localization[17]. Thus, while a great deal of information has accumulated in the last few years concerning the complexity of SMN biology, why motor neurons seem to be especially susceptible in SMA has still not been resolved[18].

SMA has recently attracted a great deal of attention from researchers because of its monogenic nature and seemingly straightforward path to the clinic. While much is not understood, data obtained from SMA patients and from SMA mouse models suggest that therapeutics that elevate SMN levels could be effective in treating this disease[19]. A very significant question, then, relates to the best way of finding and testing potential therapeutics. Several previous investigators have screened chemical diversity libraries using reporter gene assays to identify agents that either increase *SMN2* transcription[20] or correct the exon 7 splicing defect in the *SMN2* gene[21]. The advantage of this type of assay is that it can be carried out rapidly and used to screen large compound libraries. A novel type of study was conducted to find small molecule modulators of snRNP assembly in the hope of identifying compounds that might functionally replace SMN in this process[22]. Microscope-based assays have been employed much less frequently, generally in the context of validating hits identified in reporter gene screens[23]. In these cases, assays have focused on testing compounds for their ability to increase the number of nuclear gems as a “surrogate” method of ensuring that compounds could increase the amount of functional SMN. Such an assay depends on gems counts accurately reflecting the amount of active protein.

In work reported here, we have adopted a different type of approach. First, we have carried out a more complete image-based screen designed to find compounds that increase SMN in the cytoplasm, nucleus, or in nuclear gems. This unbiased approach allows us to identify cells with elevated SMN regardless of where the functional SMN might reside or how the protein was modified. We tested different sets of annotated compounds, as opposed to chemical diversity libraries, with the goal of discovering molecular targets that might be implicated in determining SMN levels, whether they increase *SMN2* transcription, correct the splicing defect or stabilize SMN protein. We further attempted to connect the various cellular targets into regulatory pathways to identify the most “druggable” components of the pathways. In this respect, our chemical biology approach can be considered to be similar to

genetic screens of the type recently published[24]. Finally, we show that small molecule inhibitors of GSK-3, one of the druggable targets downstream in a key receptor tyrosine kinase signaling pathway, increase SMN levels in SMA patient-derived fibroblasts and also in motor neurons. These molecules are able to block motor neuron death resulting from SMN knockdown, validating that our screens are capable of identifying molecules that correct true disease-specific phenotypic defects.

RESULTS

Design of an image-based SMN assay

Our main goal was to establish an assay capable of identifying compounds and, ultimately, signaling pathways that increase the amount of functional SMN protein on a per cell basis. Previous research suggests that truncated SMN (lacking exon 7 amino acids) can be functional, at least in cells that also have full-length SMN[4,25]; thus we used an antibody that recognizes both forms of SMN. We carried out our screen using small collections of annotated compounds, including those that activate or inhibit membrane receptors, channels and kinases, rather than large chemical diversity libraries. Many of our compounds have known activities, which aids in the progression from screen to target identification. Some of the molecules included in the screened collection were known drugs that potentially could be re-purposed to treat SMA. Our recent work has demonstrated the value of screening these types of compounds in related projects[26,27]. Summary of our screen is described in Supplementary Table 1.

Primary screening results

MG-132, a proteasome inhibitor previously characterized as an SMN-elevating compound[28], was used to establish basic parameters for the screen. Cultures were treated for 48 hours, fixed and stained with an anti-SMN monoclonal antibody, and then with a fluorophore-conjugated anti-mouse antibody and Hoechst 33258 to label nuclei. Cells were viewed with an automated confocal microscope. Customized image analysis software delineated nuclear and cytoplasmic compartments and finds SMN-containing gems in the search region defined by the nuclear border, as described in detail in Supplementary Methods. The intensity of SMN staining in these discrete compartments could then be quantified (Fig. 1a,b). Our assay and analysis conditions were sufficient to produce statistically significant data, including dose-response curves, for active compounds.

The workflow for our screen is summarized in Supplementary Results, Supplementary Fig. 1a,b, and a representative heat map is shown in Supplementary Fig. 1c, with scatter plots given in Fig. 1c. In all, approximately 3500 compounds were tested, each at 3 different concentrations. This is because potencies (EC_{50}) of the molecules in our library can vary from nM to greater than 10 μM. If a compound is used at concentrations in vast excess of its individual active range, its specific, or on-target, effect might be lost and the chances of encountering toxicity would become higher. Screening at multiple concentrations, ranging from low to high, maximizes the probability of testing each compound at a near-optimal point. Cytoplasmic and nuclear SMN measurements showed small variability; however, gem numbers and gem intensity gave more variable results (Fig. 1c). This is probably due to the small and diverse size of gems and their changeable number even in untreated cells. In part, it also may be attributed to the fact that gems become harder to detect as the overall nuclear "background" increases, so that compounds that produced particularly impressive increases in nuclear SMN appeared to decrease gem counts. For example, HDAC inhibitors, such as trichostatin, which scored in the screen, increased gem numbers at lower concentrations, while at higher doses, the total nuclear SMN continued to increase, but gem number appeared to decrease (Supplementary Fig. 2a,b). This further supports the notion that

interrogating both nuclear and cytoplasmic compartments, as well as gem number, might provide additional valuable information. Most of the data in this paper were derived from compounds that increased SMN levels in those two compartments, regardless of their effects on Gem numbers.

Compounds can increase SMN in cytoplasm, nucleus or gems

For the data in this paper, compounds were considered as hits if they increased SMN greater than 30% in two of the cellular compartments (cytoplasm, nucleus, gems) at any concentration. We chose 30% as the cutoff since various results suggest that this level of increase might produce a disease lessening effect. A total of 384 primary hits that increased SMN levels in parental lines were re-tested in 8-point dose-response curves, using fibroblasts derived from SMA patients. 220 compounds with confirmed activity were screened with the same assay conditions, but in the absence of the anti-SMN primary antibody, in order to eliminate fluorescent compounds. We obtained 188 confirmed hits (**Data Set 1**). These were analyzed further and clustered according to their annotated targets — e.g., receptors or enzymes to which they might bind. The pie chart in Supplementary Fig. 1d represents an analysis of the types of compounds that constituted the set of 188 confirmed hits.

We observed that, at particular times after compound addition, the SMN increase was not homogeneous in all compartments and that the effect of individual types of compounds varied as to which pool of SMN was primarily affected. Illustrations of this finding are presented in Fig. 2 and in Supplementary Fig.3. For example, at several different concentrations, both the proteasome inhibitor lactacystin and the calpain inhibitor ALLN produced an obvious increase in gem number; however the increase in overall nuclear SMN was much less dramatic. At sub-micromolar concentrations, an imidazolo-oxindole PKR inhibitor induced more than a 50% increase in cytoplasmic SMN, but a much smaller change in nuclear SMN was observed. The PDE V inhibitor MBCQ had a similar effect at concentrations ranging from 0.3–100 μM. At particular concentrations and times of treatment, both the cannabinoid agonist WIN 55,212-2 and the HDAC inhibitor SAHA produced more of an increase in the nuclear, than in the cytoplasmic, compartment. These results reinforce the value of carrying out this type of comprehensive image analysis.

Ion channel modulators increase SMN levels

We carried out a more detailed study of a small number of the compound classes that were identified and confirmed in our screen. We found that Na,K-ATPase inhibitors, such as the cardiac glycoside ouabain, consistently emerged as hits (Fig. 3, image shown in Supplementary Fig. 4a). Multiple cardiac glycosides could increase SMN in the nucleus and cytoplasm at concentrations close to those at which they are known to inhibit the enzyme[29,30] (Supplementary Fig. 4b). Mechanistically, these enzyme inhibitors should produce a net gain in intracellular Na^+ that may then lead to increased intracellular Ca^{2+} via activity of the Na,Ca-exchanger[31]. Thus, we tested compounds that directly increase Na^+ or Ca^{2+} levels. Monensin, a sodium ionophore, also increased SMN, as did the Ca^{2+} ionophore A23187 (Fig. 3, image shown in Supplementary Fig. 4a). As an alternative way of increasing Ca^{2+}, we tested thapsigargin, an inhibitor of the endoplasmic reticulum Ca^{2+}-ATPase, which stimulates release of Ca^{2+} from intracellular stores. Thapsigargin addition also resulted in SMN upregulation (Fig. 3, image shown in Supplementary Fig. 4a). Data on additional sodium and calcium elevating compounds are given in Supplementary Fig. 4c. These results demonstrate that one way in which ouabain and other Na,K-ATPase inhibitors increase SMN is by increasing intracellular calcium. The effects of Ca^{2+} increasing treatments are being explored separately.

Growth factors increase SMN levels

Recent publications have also described other ways that circulating hormone-like molecules such as ouabain may act, namely, by modulating intracellular signaling pathways, including those regulated by ligands of receptor tyrosine kinases (RTKs)[32]. We carried out a set of experiments to test if direct activation of RTKs might also be able to increase SMN levels. SMA patient fibroblasts were incubated with various RTK ligands for 72 hours and then SMN levels were measured. We found that several of them were active (Supplementary Table 2). Platelet-derived growth factor (PDGF), and in particular PDGF-BB, produced the greatest fold-increase in SMN levels, reaching more than 2-fold after 72 hrs (Fig. 4a, image shown in Supplementary Fig. 5a). Several other PDGF isoforms gave increases in nuclear and cytoplasmic SMN after 72 hours of incubation (Supplementary Fig. 5b).

To determine the specificity of PDGF action, we used a PDGF neutralizing antibody. In the experiment illustrated in Fig. 4b, we added increasingly larger amounts of antibody while keeping the PDGF concentration fixed. The increase produced by PDGF was blocked. Next, we pre-incubated cells with DMPQ or AG-1236, two small molecule PDGF receptor (PDGFR) inhibitors. As seen in Fig. 4c, at a fixed concentration of those two inhibitors, the elevated levels of SMN produced by even high levels of PDGF-BB were substantially reduced, going below baseline levels. We normally maintain our cells in serum-containing medium, which has PDGF as a component. Thus, we speculated that part of this effect could be due to additional blockade of the signaling produced by the PDGF in serum. This also appeared to be the case since either adding the PDGF neutralizing antibody or PDGFR kinase inhibitors to the medium of otherwise untreated cells (Supplementary Fig. 5c) or reducing serum from 10% to 0.5% (Supplementary Fig. 5d) could decrease SMN. We conclude that the amount of SMN per cell is responsive to physiological levels of PDGF and, presumably, of other RTK ligands.

PDGF increases SMN, in part, by inhibiting GSK-3β

With some variation from cell type to cell type, PDGF-BB is known to activate several intracellular pathways including those involving the MAP kinase cascade and PI3K/AKT signaling. To gain some information as to which downstream kinases are phosphorylated upon PDGF receptor stimulation in SMA patient fibroblasts, we used a Phospho-Mitogen-Activated Protein Kinase antibody array and compared the profile of relative phosphorylation of 19 kinases between untreated and PDGF treated samples. PDGF addition primarily led to phosphorylation of AKT, RSK1, p38 and GSKα/β, while having little effect on the phosphorylation of ERK1 and ERK2 or most other kinases under our treatment conditions (Supplementary Fig. 6a,b).

In order to illuminate which pathways downstream of the PDGFR are responsible for SMN regulation, we treated cells with inhibitors of downstream kinases prior to PDGF stimulation. Consistent with the failure to find substantial modification of ERK1/2 phosphorylation after PDGF addition, we observed that the ERK1/2 kinase inhibitors PD98059 and U0126 produced, at best, a partial inhibition of the PDGF effect (Supplementary Fig. 7a,b). Pre-treatment of cells with either of two structurally distinct p38 inhibitors, SB202190 (Supplementary Fig. 7c,d) or SB203580, yielded a moderate inhibition of SMN in the cytoplasm, but did not inhibit nuclear SMN. However, the PDGF-mediated SMN increase could be completely abolished by addition of a PI3K inhibitor LY294002 (Fig. 5a,b). Additionally, the SMN increase was abolished by PI-103, a dual inhibitor of PI3K and mTOR (Fig. 5b). If PI3K transmits the PDGF signal, we would also expect PI3K inhibitors to decrease the basal level of SMN when cells are kept in their normal serum-containing medium. This turned out to be the case: addition of chemically different PI3K

inhibitors to cells caused as much as a 20–40% reduction in SMN levels in nucleus and cytoplasm (Supplementary Fig. 7e,f).

These results suggest that RTK ligands, such as PDGF, regulate SMN levels using a signal transduction cascade initiated by activation of PI3K. To further explore this finding, we examined the role of GSK-3, a constitutively active kinase downstream of PDGFR and PI3K/AKT. First, we confirmed by Western blot analysis that PDGF increases SMN relative to tubulin (Fig. 5c,d), (the full gel is shown in Supplementary Fig.8a). The fold increase seen by Western blot was similar to that observed by imaging, even though the measurements are somewhat different in that SMN as measured by cellular imaging is not normalized with respect to the levels of other proteins. This demonstrates that the effects of PDGF do not result from a global increase in cellular protein. It is known that phosphorylation of GSK-3β on Ser-9 or of GSK-3α on Ser21 residues leads to inhibition of enzyme activity[33,34]. This inhibition is produced by RTK and Wnt signaling and results in activation of downstream targets. We next prepared cellular lysates from patient fibroblasts that were stimulated with 50ng/ml of PDGF-BB for 1 hour. Western blot analysis showed that PDGF increased the inhibitory phosphorylation of both GSK-3β and GSK-3α (Fig. 5c), (the full gels are shown in Supplementary Fig.8b,c). Immunocytochemistry experiments confirmed a dose-dependent increase of the phosphorylated form of the GSK-3β enzyme at 72 hours (Supplementary Fig. 8d). The localization of phospho-Ser9-GSK in PDGF-treated fibroblasts bears a superficial resemblance to the staining pattern for SMN itself (Supplementary Fig. 8e). A careful examination found, however, that the distribution of p-GSK-Ser9 did not overlap completely with that of SMN (Supplementary Fig. 8f). Further study will be necessary to see if there is meaningful co-localization of GSK-3β and SMN in any intracellular compartment.

Having confirmed that PDGF addition can lead to phosphorylation and, hence, inhibition of GSK-3 kinase, we explored whether GSK-3 is functionally important in controlling SMN. We tested several different chemical inhibitors of this enzyme for their effects on SMN levels. At relatively low concentrations, alsterpaullone (Fig. 6a,b), a dual GSK-3, cyclin-dependent kinase inhibitor, and to a lesser extent its analog 2-cyanoethyl alsterpaullone[35] (Avg for 3-day treatement is 1.67+/−0.19 in 2 separate experiments) were able to elevate SMN in patient fibroblasts. We also tested an extensive list of other putative GSK kinase inhibitors and found several additional inhibitors that were able to increase SMN (Supplementary Fig. 9a,b).

To confirm that the compounds were acting, at least in part, as GSK-3 inhibitors, we treated patient fibroblasts with lentiviruses containing anti-GSK shRNA constructs. There are two GSK-3 isoforms, α and β, which, although they may differ somewhat in their cellular actions, have virtually identical catalytic sites and both are likely to be inhibited by the compounds we used[36]. We reduced the levels of the two isoforms singly and in combination. We found a significant increase in SMN levels in cells with less GSK-3 protein, observing as much as 4–5-fold increase in the double knockdown cells (Fig. 6c,d), (the full gels are shown in Supplementary Fig. 9c–e). This result validates GSK-3 kinase as a true molecular regulator of SMN.

GSK-3 inhibitors reduce the rate of SMN degradation

We were interested in determining how activation of RTK signaling pathways and inhibition of GSK-3 might produce higher cellular concentrations of SMN. In other words, we wanted to determine if their actions could be accounted for by (a) increasing *SMN2* transcription, (b) changing the degree of splicing to produce more full-length mRNA, or (c) stabilizing existing protein. First, we used q-PCR to measure the levels of truncated and full-length mRNAs at various times after treatment using conditions identical to those that increase

protein levels. Particularly at earlier time points, we found a relatively small and variable increase (approximately 2-fold) in full-length or in truncated mRNA levels, depending on the treatment (Supplementary Fig. 10a,b). In any case, in no instance did we find a striking change in splicing alone (i.e., a shift in the proportion of mRNA that was full-length).

Therefore, we also considered an effect on protein stability, especially since proteasome inhibitors score consistently in our assay and GSK-3 is a known regulator of protein stability[37]. Importantly, SMN has a consensus GSK-3 phosphorylation site on Ser4[38,39] and we confirmed by mass spectroscopy analysis that this residue is phosphorylated in untreated cells (Supplementary Fig. 11). Expressing a tagged S4D mutant SMN protein or tagged S4D mutant Δ7 SMN led to a significant decrease in protein levels compared to expressing tagged forms of wildtype SMN or Δ7 SMN, respectively (Figure 7a,b), consistent with the notion that both forms of the protein degrade more rapidly when this residue is phosphorylated. As further confirmation, we expressed tagged versions of these mutant forms in HEK cells, treated them with cycloheximide to inhibit protein synthesis and measured SMN levels over the next 12 hour period[40]. The turnover rates of the S4D mutants were much more rapid, particularly for the Δ7 form (Figure 7c–f), (the full gels are shown in Supplementary Fig. 12a–d). Thus, GSK-3 appears to phosphorylate SMN and increase its turnover rate, leading to a decrease in total levels. The enzyme inhibitors may act by reducing the level of SMN phosphorylation, producing an increase in stability.

Alsterpaullone rescues motor neurons after Smn knockdown

Our screen revealed many distinct classes of compounds that are capable of elevating SMN in different intracellular compartments. Because it is not entirely clear where the functional SMN resides (and whether the functional SMN has particular post-translational modifications), we felt that it was important to determine if any of these compounds could exert a positive effect on a cell type relevant to understanding and treating SMA. We chose to investigate whether GSK-3 kinase inhibitors could promote survival of mouse motor neurons with reduced Smn levels. It is important to note that PDGF itself has no effect on SMN levels in motor neurons. Gene expression analysis of our motor neurons confirms that these cells are relatively deficient in PDGFRs compared to fibroblasts.

Motor neurons were produced from mouse ES-cells expressing cherry fluorescent protein (CFP) under the control of the motor neuron-selective Hb9 promoter, as previously described[41]. We first used single cell imaging to confirm that alsterpaullone could elevate Smn in motor neurons (Fig. 8a). Alsterpaullone did increase SMN (Avg for a 3-day treatment is 1.69+/−0.12 in 4 separate experiments; range of increase was 1.5–1.8-fold). While the effect was somewhat smaller than what we found in human fibroblasts, it is in the range of what we have found with other compounds that increase motor neuron SMN and in the range of increases anticipated to have an impact on disease progression (in preparation).

Wildtype motor neurons were infected with three lentiviral constructs acquired from Open Biosystems (pGIPZ): a non-silencing (NS) shRNA and two with unique shRNA sequences directed against the *Smn* transcript. Virtually all of the motor neurons were infected under the conditions chosen for these experiments. Quantification of SMN knockdown was first performed using 3T3 cells with Puromycin selection (Supplementary Fig. 13a,b). Both lentiviral shRNA constructs reduced Smn levels, but Smn-shRNA#2 was more effective. We then checked the three lentiviral constructs in motor neurons by sorting ES cell-derived motor neurons (cherry positive cells) infected with the pGIPZ lentiviruses (GFP positive cells) by FACS and quantifying the amount of SMN by Western blot. Uninfected and NS pGIPZ infected motor neurons had approximately the same level of SMN. In contrast, both sets of Smn-shRNA infected motor neurons had a greater than 65% knockdown, with Smn-

shRNA#2 again reducing Smn levels to a larger degree (Supplementary Fig. 13c,d). Subsequent work was carried out with that more effective lentiviral construct.

We performed motor neuron survival assays to test the effects of reduced levels of Smn. Motor neurons were plated and left untreated or infected with either the NS shRNA or Smn#2 shRNA on DIV 1. Three days post-infection (DIV 4), although there is a decrease in the motor neurons over this period, there was no difference in number of cells between untreated motor neurons and those infected with the non-silencing lentivirus. However, there was a significant reduction in motor neuron numbers in cells with lower SMN (Fig. 8b). Therefore, motor neurons with an average level of SMN less than 30% that of wildtype experienced a significantly higher level of cell death. These results show, as might be expected, that reducing SMN compromises motor neuron survival.

To test the effects of SMN increasing compounds, we added them to motor neurons two days after lentiviral infection. Over the course of the subsequent three days, we counted live cherry expressing motor neurons on a daily basis. In the presence of alsterpaullone, the survival of motor neurons after SMN knockdown was similar to that of control wildtype cells either untreated or treated with alsterpaullone (Fig. 8c and Supplementary Fig. 13e,f) and much greater than that of infected motor neurons not receiving compound. In other words, alsterpaullone was able to block virtually all of the death that was attributable to acute reduction in SMN. Alsterpaullone did not, however, block the basal level of cell death seen in all of the motor neuron cultures and, hence, did not have a general survival promoting effect on motor neurons.

DISCUSSION

Even though the mutations that underlie SMA, a serious childhood genetic disease of motor neurons, are now well known, the disease is still not completely understood. In particular, why motor neurons die selectively when SMN levels decrease below a certain threshold remains unclear, also providing uncertainty as to whether the functional protein in motor neurons is the SMN found in nuclear gems or, for example, in the axon. However, what does seem clear is that the severity of the disease diminishes as the number of copies of the *SMN2* gene increases. That further suggests that higher levels of functional protein will also lead to improvement in the course of the disease. Therefore, we carried out a cell-based screen designed to identify compounds that increase SMN anywhere within cells, rather than just in gems. In addition, we established an additional assay in which SMN-elevating compounds could be tested for their ability to correct a phenotypic defect associated with the disease. In experiments included here, we chose motor neuron death caused by lentiviral knockdown of Smn.

We tested collections of annotated bioactive molecules, rather than diverse compound sets. Our rationale for doing this is that one of our main objectives was to identify SMN regulatory pathways that might lead us to the identification of receptors or enzymes that could be targeted to treat SMA. Our image-based screening was probably more difficult to carry out than a standard reporter gene assay, but, nonetheless, we identified numerous reproducible hits that increased SMN levels quite significantly in SMA patient fibroblasts. Hits from our screen fell into a variety of classes, some of which are described in more detail in this paper. We found that relatively low concentrations of various Na,K-ATPase inhibitors scored consistently. Part of the effect of this compound class could be attributed to the increased intracellular Na^+ and Ca^{2+} that accompanies inhibition of that membrane transporter. However, part of the effect of Na,K-ATPase inhibitors may also be explained by the ability of cardiac glycosides such as ouabain to activate intracellular signaling pathways downstream of RTKs. To probe these pathways, we treated fibroblasts with different RTK

ligands and found many of them to be active as well, with PDGF-BB producing the greatest level of increase. SMN levels were very responsive to changes in PDGF concentrations in the cell culture medium. PDGF addition elevated SMN, while resting levels of SMN could be decreased significantly by blocking endogenous PDGF in serum (or simply reducing the amount of serum in the cell culture medium). This suggests that RTK ligands, such as PDGF, might control SMN levels under normal cell growth conditions.

Since several growth factors increased cell numbers in addition to SMN levels, there is some chance that those two processes are inextricably linked. That is, perhaps SMN levels simply increase when cells are subjected to a mitogenic stimulus. However, this cannot be the entire explanation for our results since many of the molecules that induce cells to produce more SMN actually decrease cell numbers rather dramatically. For example, this is readily seen with both HDAC inhibitors and proteasome inhibitors, which are well known to have cytostatic or anti-proliferative effects. Furthermore, some of the hits from this fibroblast screen are also effective on motor neurons, which are clearly incapable of proliferating. Thus, there is no absolute connection between SMN levels and the cell cycle. Nonetheless, it is also true that we and others have found that C2C12 cells[42] proliferate relatively slowly, while neurospheres with low levels of SMN proliferate faster[43]. So, under certain circumstances elevated SMN levels may play a role in, or be responsive to, the cell division process.

Based on a phosphoproteomic analysis, PDGF was seen to be associated with activation of PI3K/AKT/GSK-3-mediated signaling, with some activation of RSK. The cells also appeared to have activated p38, normally considered to be regulated by stress[44], rather than by growth factors like PDGF. We did find that anisomycin, a p38 activator, scored in our screen, suggesting that this pathway can modulate SMN levels. A recent report also found anisomycin could rapidly increase SMN levels, apparently by stabilizing and increasing mRNA levels[45]. However, we found that both ERK and p38 inhibitors had a relatively minor ability to block the increase in SMN that followed PDGF treatment. In contrast, PI3K antagonists had a strong inhibitory effect, suggesting that this is a major arm of the SMN regulatory pathway. Consistent with that was our demonstration that PDGF addition also led to an increase in Ser-9 and Ser21 phosphorylation of GSK-3α and β in our cells, thereby inhibiting that enzyme. Treating cells with a variety of chemical GSK-3β inhibitors produced an elevation of cellular SMN. We confirmed that some of the activity of the inhibitors is likely to be due to inhibition of GSK-3. Reducing levels of GSK-3α and β individually or together using shRNAs produced an extremely impressive increase in SMN levels in patient fibroblasts. This suggests that chemical enzyme inhibitors more potent or specific than the ones we used might also produce even a larger increase in SMN.

PDGF and some GSK-3 inhibitors increased SMN levels without yielding a consistent or dramatic increase in mRNA or a change in splicing. Given that proteasome inhibitors, which act to block protein degradation, also increased SMN, one possibility is that PDGF and its downstream mediator GSK-3β increase SMN by blocking its degradation. Interestingly, there is a consensus GSK-3 phosphorylation site on Ser4 of SMN. Using mass spectrometry, we confirmed that this site in phosphorylated in our cells, but a more detailed study will be needed to explore SMN posttranslational modifications quantitatively. Furthermore, recent data suggest that phosphorylation by GSK-3, which has a well-documented role in mediating degradation of β-catenin in the Wnt signaling pathway[33], may have a broader role in regulating turnover of a variety of intracellular proteins[37]. Therefore, we hypothesized that RTK signaling inhibits GSK-3, decreasing its phosphorylation of SMN, thereby slowing Smn degradation. This was confirmed using mutagenesis experiments in which we showed that replacing Ser4 with an aspartic acid residue, mimicking a state of chronic phosphorylation, causes a sharp increase in the degradation rate of SMN.

In order to confirm that the hits we discovered had SMA-relevant biological activity, we were interested in establishing an appropriate phenotypic assay. Since SMA is a disease that involves motor neuron dysfunction and death, we focused on setting up a motor neuron assay. Previously, we isolated ES cells from a mouse model of SMA and found that motor neurons produced from these ES cells die soon after differentiation (Sinor-Anderson et al., in preparation). However, for studies described here, we chose a model in which lentiviral shRNA was used to reduce SMN in wildtype ES cell-derived motor neurons. One important issue relates to whether this is a valid phenotypic assay to test SMN-elevating compounds for their potential usefulness. It is well known that all cells require SMN and cannot proliferate or survive if their SMN is reduced sufficiently. Under the conditions of our experiments, motor neurons were selectively infected with the lentiviral vector and hence died preferentially compared to other cells in the culture, but not until their levels of SMN were reduced by approximately 75%. By way of comparison, in cultures in which SMN-deficient mouse ES are induced to differentiate into motor neurons and glial cells, motor neurons die rapidly, as mentioned, but glial cells are relatively unaffected. Therefore, that while the cell death that we observed following lowering of SMN may not be absolutely specific to motor neurons, it can nonetheless form the basis of an assay capable of choosing compounds that can modify the neurodegenerative changes that constitute the pathological basis of SMA.

PDGF itself did not affect either SMN levels or survival of the motor neurons, which lack PDGF receptors[46]. However, GSK-3 chemical inhibitors did increase SMN in motor neurons and rescued virtually all of the death that was seen in the motor neurons with lower Smn. In contrast, while HDAC inhibitors and various proteasome inhibitors can elevate SMN levels in ES cell-derived motor neurons, both classes of compounds are relatively toxic over the course of the survival experiments described here and neither is able to provide any phenotypic rescue. Jablonka et al. (2009) also found that the HDAC inhibitor valproic acid had negative effects on motor neurons[47]. Some of our data suggest that the most effective compounds, such as alsterpaullone, may inhibit one or more other kinases and this may contribute to their effectiveness. Future work will be directed at identifying these other kinases.

It is worthwhile pointing out that some of the commercially available GSK-3 inhibitors, with several different chemical scaffolds, were quite effective in elevating SMN in fibroblasts and motor neurons and some were not. There are several possible explanations for this. One is that most of these inhibitors are likely to affect more than one kinase[48], and it may be that there are kinases other than GSK-3α and β that play a role in SMN regulation. It will be important to determine which kinase inhibition profile correlates best with the ability to increase SMN and to use that information as part of a chemical optimization campaign to maximize the beneficial effects of using these compounds therapeutically (for example, there are some negative activities associated with alsterpaullone addition to Jurkat cells)[49]. It is also interesting to note that GSK-3 has been shown to have anti-apoptotic effects on different neuronal populations[50]. Determining whether any part of the survival promoting effect that GSK-3 inhibitors have on motor neurons is independent of SMN levels is essential (although we did not find that they enhanced motor neuron survival in general under the conditions of our experiment), as is investigating whether some of the pro-survival effects on other neurons might, unexpectedly, be modulated, in part, by increased SMN levels.

In summary, we have carried out an image-based screen of annotated collections to find compounds that increase SMN in any intracellular compartment in fibroblasts. We found more than 150 active compounds that fell into different categories. Some, but not all, of these compounds also increase Smn in motor neurons, confirming that it is not absolutely

essential to carry out primary screens in motor neurons themselves. Included among the hits were several signal transduction pathways, one of which lies downstream of membrane RTKs. GSK-3 appears to be a particularly important druggable intracellular target and inhibitors of that enzyme not only increase SMN, but rescue motor neuron death. We believe that this is the first time that an SMA screen has produced compounds that have such a striking effect on an important component of the disease. Future work will be directed at testing GSK-3 inhibitors and other modulators of intracellular signaling in mouse models of SMA.

METHODS

Culture of fibroblasts derived from patients with SMA and parental carriers

Untransformed human fibroblasts – GM09677, derived from 2-year old patient with SMA type 1 disease, and GM03814, derived from unaffected unmatched parental SMA carrier (Coriell Cell Repositories) – were grown in MEM (Invitrogen) containing 5% FBS (Invitrogen), 2 mM glutamine and penicillin-streptomycin(100 U/ml) in 5% CO_2 at 37°C.

High-content screen

Fibroblasts from parental SMA carriers were seeded at 500 cells per well in 384-well plates and treated in duplicate at 10 μM, 1 μM and 0.1 μM with individual compounds from the screening library: LOPAC^{1280} Collection (Sigma-Aldrich), Spectrum Collection (Microsource Discovery Systems), Prestwick Chemical Library, and a custom set of 289 chemicals affecting kinases, ion channels and neuroactive small molecules. After 48h, plates were stained with Hoechst and an anti-SMN antibody and scanned by an automated confocal microscope (PerkinElmer Opera) at 20X magnification with separate fluorescent exposures with a UV light source and a 488 nM laser. Image analysis was done using Opera software, by first recognizing and outlining nuclei on the basis of Hoechst staining, then by using SMN antibody staining to detect the cytoplasmic region outside of the nucleus and to allow us to define cell boundaries. Gems were then defined as “spots” within the nuclear boundaries. Finally, SMN in these three separate compartments was quantified. The average intensity of SMN per cell for the parameters of interest was calculated based on at least 10 random fields captured per well. More details are presented in Supplementary Methods. Hit compounds were defined as those that scored 1.3 fold above the DMSO control in duplicate and increased SMN in at least 2 of the following measures: cytoplasm, nucleus, the number of gems, or SMN intensity in gems. 1 μM MG-132 was used as the positive control. The HCS data were further coupled with compound structures and analyzed using the IDBS Inc. Activity Base (version 7.1) software. Hit compounds identified in the screen were further tested in an 8-point dose response in triplicate (30–0.03 μM range, at 3-fold dilutions) with identical assay conditions.

Screening reagents

Thapsigargin, A23187, WIN 55,212-2, MBCQ, ouabain, monensin, lactacystin, ALLN, AG-1296, SDZ-201106, digoxin, digitoxin, Lanatoside C, buffalin (Enzo Life Sciences); PD98059, U0126, SB203580, SB202190, DMPQ hydrochloride, PI-103, LY294002, ionomycin (Tocris); alsterpaullone and 2-cyanoethyl alsterpaullone, trichostatin (EMD Chemicals); AR-0A14418 (Sigma-Aldrich); CHIR98014 (Axon Medchem), growth factors, and neutralizing antibodies (R&D Systems) were prepared accordingly to the manufacturer’s instructions.

Immunostaining

Fibroblasts were fixed with 4% (v/v) PFA solution (Electron Microscopy Sciences) or ice-cold methanol/acetone mix (1:1) (Sigma-Aldrich) for 10 minutes. Motor neurons were fixed in methanol and stained with an Alexa 647 conjugated anti-GFP antibody to convert the GFP signal to the far-red channel. Immunostaining was carried out using standard protocols. The following primary antibodies were used: mouse anti-SMN antibodies (1:200, BD Biosciences, bulk order) and rabbit anti-p-GSK3β (Ser9) antibodies (1:300, Santa Cruz Biotechnology). Alexa 488 (Invitrogen) conjugated antibody against mouse and rabbit were used at 1:2000 dilution and followed by nuclear dye Hoechst 33342 (1:5000, Invitrogen).

qPCR

RNA was purified using the Tri-Reagent protocol (Sigma-Aldrich) and quantified on a Nanodrop (Thermo Fisher Scientific). Reverse transcription was performed on 500ng of total RNA by Superscript®VILO™cDNA kit (Invitrogen) on a Thermocycler (Bio-Rad Laboratories). qPCR was done with RT^{2}SYBR Green/ROX PCR Master Mix (SA Biosciences) on a 7900HT Fast Real-Time PCR System (Applied Biosystems). Conditions and primer sequences are described in Supplementary Methods.

Immunoblot analysis and Phospho-Kinase Array

Cells were lysed with RIPA buffer (Thermo Scientific) containing an inhibitor cocktail (VWR), and 20 μg of protein, measured by DC assay (Bio-Rad), was resolved on a 10% Tris-Glycine gel and transferred to PVDF membranes (Invitrogen) by semi-dry transfer (Bio-Rad). Primary antibodies used include mouse anti-SMN (1:10,000, BD Biosciences), rabbit anti-pGSK-3β (Ser9) (1:1000, Santa Cruz Biotechnology), rabbit anti-pGSK-3α (S21) (1:1000, Cell Signaling Technology), or anti-human β-tubulin (1:10,000, Abcam) anti-HA (1:2000 Roche). Secondary HRP–conjugated goat antibodies used were against mouse and rabbit (Thermo Scientific). Signals were enhanced using a chemiluminescence kit (West Pico Reagent) and captured by a ChemiDoc imager (Bio-Rad).

For the Phospho-Kinase Array, lysates were hybridized with membranes containing 46 pre-arrayed antibodies against different kinase phosphorylation sites (R&D Systems), following the manufacturer's protocol. Levels of chemiluminescence for each phosphorylated protein were detected by measurement on X-ray film (Kodak).

Lentivirus preparation and shRNA construct validation

Lentivirus was produced by transient co-transfection of HEK 293T17 cells with PAX2, pMD2G and pGIPZ constructs containing Smn-targeting or non-silencing shRNA (Open Biosystems) using lipofectamine (Invitrogen). Virus was concentrated with 100kDa filter Amicon Ultra-15 centrifugation units. Virus was titered using HEK 293T17 cells. The percent of SMN-knockdown was determined by western blotting of puromycin selected 3T3 cells or FACS-sorted HB9-CFP motor neurons. Lentiviral constructs for GSK knockdown, hGSK3α: TRCN0000039766 and TRCN0000038680, hGSK3β: TRCN0000039564 and TRCN0000039565 (Sigma) were produced as mentioned above.

mES cell culture and differentiation

Mouse Hb9::CFP (cherry fluorescent protein) (gift from Kevin Eggan, Harvard University) or Hb9::GFP ES cells were differentiated into motor neurons as previously described[41]. Briefly, ESC colonies were dissociated and cultured in DFNK medium. After 2 days, EBs were treated with retinoic acid (RAc; 100nM, Sigma-Aldrich) and a hedgehog agonist (100nM). On day 3, EBs were treated with RAc (100nM) and the hedgehog agonist (1 μM) and incubated for 72h. Papain (Worthington Biochemical) and DNase I (Worthington

Biochemical) were used to dissociate EBs. Cells were plated on poly-ornithine coated plates (VWR) and cultured in DMEM-F12 medium (Invitrogen) containing 2% FBS (Invitrogen), B-27 supplement (Invitrogen), 20ng/ml GDNF and BDNF, CNTF (R&D Systems), insulin, progesterone, BSA, selenite and apotransferrin (Sigma-Aldrich).

For MN survival assays, dissociated EB cultures were infected with the NS shRNA, or SMN shRNA viruses on DIV1. Compounds were added on DIV3. Percentage of MN survival was calculated compared to uninfected DMSO-treated cultures, with MN numbers obtained from the images taken during DIV3-7.

SMN stability assay

HEK 293T17 cells were transfected as described above with full length or Δ7SMN constructs. After 60 hours 100 μg/ml cycloheximide was added, and time points were collected at the indicated intervals.

Supplementary Material

Refer to Web version on PubMed Central for supplementary material.

Acknowledgments

The authors would like to thank Karen Kotkow, Yin Miranda Yang and Karen Chen for helpful comments, Katie Krumholz for a great deal of technical help and Jane LaLonde for editorial assistance. Additionally, we would like to thank Rajeev Sivasankaran and Cheng Song at Novartis for sharing the conditions of the splicing assay design. The work was supported by the Spinal Muscular Atrophy Foundation, by the Harvard Stem Cell Institute and by a P01 grant (P01NS066888-01A1) from the NINDS.

References

1. Lefebvre S, et al. Identification and characterization of a spinal muscular atrophy-determining gene. Cell. 1995; 80:155–65. [PubMed: 7813012]
2. Lefebvre S, et al. Correlation between severity and SMN protein level in spinal muscular atrophy. Nat Genet. 1997; 16:265–9. [PubMed: 9207792]
3. Lorson CL, Hahnen E, Androphy EJ, Wirth B. A single nucleotide in the SMN gene regulates splicing and is responsible for spinal muscular atrophy. Proc Natl Acad Sci U S A. 1999; 96:6307–11. [PubMed: 10339583]
4. Le TT, et al. SMNDelta7, the major product of the centromeric survival motor neuron (SMN2) gene, extends survival in mice with spinal muscular atrophy and associates with full-length SMN. Hum Mol Genet. 2005; 14:845–57. [PubMed: 15703193]
5. Patrizi AL, et al. SMN protein analysis in fibroblast, amniocyte and CVS cultures from spinal muscular atrophy patients and its relevance for diagnosis. Eur J Hum Genet. 1999; 7:301–9. [PubMed: 10234506]
6. Nguyen thi M, et al. A two-site ELISA can quantify upregulation of SMN protein by drugs for spinal muscular atrophy. Neurology. 2008; 71:1757–63.
7. Schrank B, et al. Inactivation of the survival motor neuron gene, a candidate gene for human spinal muscular atrophy, leads to massive cell death in early mouse embryos. Proc Natl Acad Sci U S A. 1997; 94:9920–5. [PubMed: 9275227]
8. Zhang Z, et al. SMN deficiency causes tissue-specific perturbations in the repertoire of snRNAs and widespread defects in splicing. Cell. 2008; 133:585–600. [PubMed: 18485868]
9. Liu Q, Dreyfuss G. A novel nuclear structure containing the survival of motor neurons protein. Embo J. 1996; 15:3555–65. [PubMed: 8670859]
10. Pellizzoni L, Kataoka N, Charroux B, Dreyfuss G. A novel function for SMN, the spinal muscular atrophy disease gene product, in pre-mRNA splicing. Cell. 1998; 95:615–24. [PubMed: 9845364]

11. Konig H, Matter N, Bader R, Thiele W, Muller F. Splicing segregation: the minor spliceosome acts outside the nucleus and controls cell proliferation. Cell. 2007; 131:718–29. [PubMed: 18022366]
12. Pessa HK, et al. Minor spliceosome components are predominantly localized in the nucleus. Proc Natl Acad Sci U S A. 2008; 105:8655–60. [PubMed: 18559850]
13. Steitz JA, et al. Where in the cell is the minor spliceosome? Proc Natl Acad Sci U S A. 2008; 105:8485–6. [PubMed: 18562285]
14. Rossoll W, et al. Smn, the spinal muscular atrophy-determining gene product, modulates axon growth and localization of beta-actin mRNA in growth cones of motoneurons. J Cell Biol. 2003; 163:801–12. [PubMed: 14623865]
15. Zhang H, et al. Multiprotein complexes of the survival of motor neuron protein SMN with Gemins traffic to neuronal processes and growth cones of motor neurons. J Neurosci. 2006; 26:8622–32. [PubMed: 16914688]
16. McWhorter ML, Monani UR, Burghes AH, Beattie CE. Knockdown of the survival motor neuron (Smn) protein in zebrafish causes defects in motor axon outgrowth and pathfinding. J Cell Biol. 2003; 162:919–31. [PubMed: 12952942]
17. Jablonka S, Beck M, Lechner BD, Mayer C, Sendtner M. Defective Ca2+ channel clustering in axon terminals disturbs excitability in motoneurons in spinal muscular atrophy. J Cell Biol. 2007; 179:139–49. [PubMed: 17923533]
18. Burghes AH, Beattie CE. Spinal muscular atrophy: why do low levels of survival motor neuron protein make motor neurons sick? Nat Rev Neurosci. 2009; 10:597–609. [PubMed: 19584893]
19. Avila AM, et al. Trichostatin A increases SMN expression and survival in a mouse model of spinal muscular atrophy. J Clin Invest. 2007; 117:659–71. [PubMed: 17318264]
20. Jarecki J, et al. Diverse small-molecule modulators of SMN expression found by high-throughput compound screening: early leads towards a therapeutic for spinal muscular atrophy. Hum Mol Genet. 2005; 14:2003–18. [PubMed: 15944201]
21. Andreassi C, et al. Aclarubicin treatment restores SMN levels to cells derived from type I spinal muscular atrophy patients. Hum Mol Genet. 2001; 10:2841–9. [PubMed: 11734549]
22. Wan L, Ottinger E, Cho S, Dreyfuss G. Inactivation of the SMN complex by oxidative stress. Mol Cell. 2008; 31:244–54. [PubMed: 18657506]
23. Mattis VB, et al. Novel aminoglycosides increase SMN levels in spinal muscular atrophy fibroblasts. Hum Genet. 2006; 120:589–601. [PubMed: 16951947]
24. Chang HC, et al. Modeling spinal muscular atrophy in Drosophila. PLoS One. 2008; 3:e3209. [PubMed: 18791638]
25. Burnett BG, et al. Regulation of SMN protein stability. Mol Cell Biol. 2009; 29:1107–15. [PubMed: 19103745]
26. Chen S, et al. A small molecule that directs differentiation of human ESCs into the pancreatic lineage. Nat Chem Biol. 2009; 5:258–65. [PubMed: 19287398]
27. Ichida JK, et al. A small-molecule inhibitor of tgf-Beta signaling replaces sox2 in reprogramming by inducing nanog. Cell Stem Cell. 2009; 5:491–503. [PubMed: 19818703]
28. Chang HC, Hung WC, Chuang YJ, Jong YJ. Degradation of survival motor neuron (SMN) protein is mediated via the ubiquitin/proteasome pathway. Neurochem Int. 2004; 45:1107–12. [PubMed: 15337310]
29. Pullen MA, Brooks DP, Edwards RM. Characterization of the neutralizing activity of digoxin-specific Fab toward ouabain-like steroids. J Pharmacol Exp Ther. 2004; 310:319–25. [PubMed: 14982968]
30. Dodson AW, Taylor TJ, Knipe DM, Coen DM. Inhibitors of the sodium potassium ATPase that impair herpes simplex virus replication identified via a chemical screening approach. Virology. 2007; 366:340–8. [PubMed: 17544048]
31. Burt JM, Langer GA. Ca++ distribution after Na+ pump inhibition in cultured neonatal rat myocardial cells. Circ Res. 1982; 51:543–50. [PubMed: 6216020]
32. Wasserstrom JA, Aistrup GL. Digitalis: new actions for an old drug. Am J Physiol Heart Circ Physiol. 2005; 289:H1781–93. [PubMed: 16219807]

33. Cohen P, Goedert M. GSK3 inhibitors: development and therapeutic potential. Nat Rev Drug Discov. 2004; 3:479–87. [PubMed: 15173837]
34. Fang X, et al. Phosphorylation and inactivation of glycogen synthase kinase 3 by protein kinase A. Proc Natl Acad Sci U S A. 2000; 97:11960–5. [PubMed: 11035810]
35. Kunick C, et al. Structure-aided optimization of kinase inhibitors derived from alsterpaullone. Chembiochem. 2005; 6:541–9. [PubMed: 15696597]
36. Cheng H, Woodgett J, Maamari M, Force T. Targeting GSK-3 family members in the heart: A very sharp double-edged sword. J Mol Cell Cardiol. [PubMed: 21163265]
37. Xu C, Kim NG, Gumbiner BM. Regulation of protein stability by GSK3 mediated phosphorylation. Cell Cycle. 2009; 8:4032–9. [PubMed: 19923896]
38. Pearson RB, Kemp BE. Protein kinase phosphorylation site sequences and consensus specificity motifs: tabulations. Methods Enzymol. 1991; 200:62–81. [PubMed: 1956339]
39. Badorff C, Seeger FH, Zeiher AM, Dimmeler S. Glycogen synthase kinase 3beta inhibits myocardin-dependent transcription and hypertrophy induction through site-specific phosphorylation. Circ Res. 2005; 97:645–54. [PubMed: 16141410]
40. Cho S, Dreyfuss G. A degron created by SMN2 exon 7 skipping is a principal contributor to spinal muscular atrophy severity. Genes Dev. 24:438–42. [PubMed: 20194437]
41. Wichterle H, Lieberam I, Porter JA, Jessell TM. Directed differentiation of embryonic stem cells into motor neurons. Cell. 2002; 110:385–97. [PubMed: 12176325]
42. Shafey D, Cote PD, Kothary R. Hypomorphic Smn knockdown C2C12 myoblasts reveal intrinsic defects in myoblast fusion and myotube morphology. Exp Cell Res. 2005; 311:49–61. [PubMed: 16219305]
43. Shafey D, MacKenzie AE, Kothary R. Neurodevelopmental abnormalities in neurosphere-derived neural stem cells from SMN-depleted mice. J Neurosci Res. 2008; 86:2839–47. [PubMed: 18521935]
44. Pearson G, et al. Mitogen-activated protein (MAP) kinase pathways: regulation and physiological functions. Endocr Rev. 2001; 22:153–83. [PubMed: 11294822]
45. Farooq F, Balabanian S, Liu X, Holcik M, MacKenzie A. p38 Mitogen-activated protein kinase stabilizes SMN mRNA through RNA binding protein HuR. Hum Mol Genet. 2009; 18:4035–45. [PubMed: 19648294]
46. Yeh HJ, et al. Developmental expression of the platelet-derived growth factor alpha-receptor gene in mammalian central nervous system. Proc Natl Acad Sci U S A. 1993; 90:1952–6. [PubMed: 8446614]
47. Rak K, et al. Valproic acid blocks excitability in SMA type I mouse motor neurons. Neurobiol Dis. 2009; 36:477–87. [PubMed: 19733665]
48. Bain J, et al. The selectivity of protein kinase inhibitors: a further update. Biochem J. 2007; 408:297–315. [PubMed: 17850214]
49. Lahusen T, De Siervi A, Kunick C, Senderowicz AM. Alsterpaullone, a novel cyclin-dependent kinase inhibitor, induces apoptosis by activation of caspase-9 due to perturbation in mitochondrial membrane potential. Mol Carcinog. 2003; 36:183–94. [PubMed: 12669310]
50. Takadera T, Ohtsuka M, Aoki H. Chelation of Extracellular Calcium-Induced Cell Death was Prevented by Glycogen Synthase Kinase-3 Inhibitors in PC12 Cells. Cell Mol Neurobiol. 2009 [PubMed: 19688259]

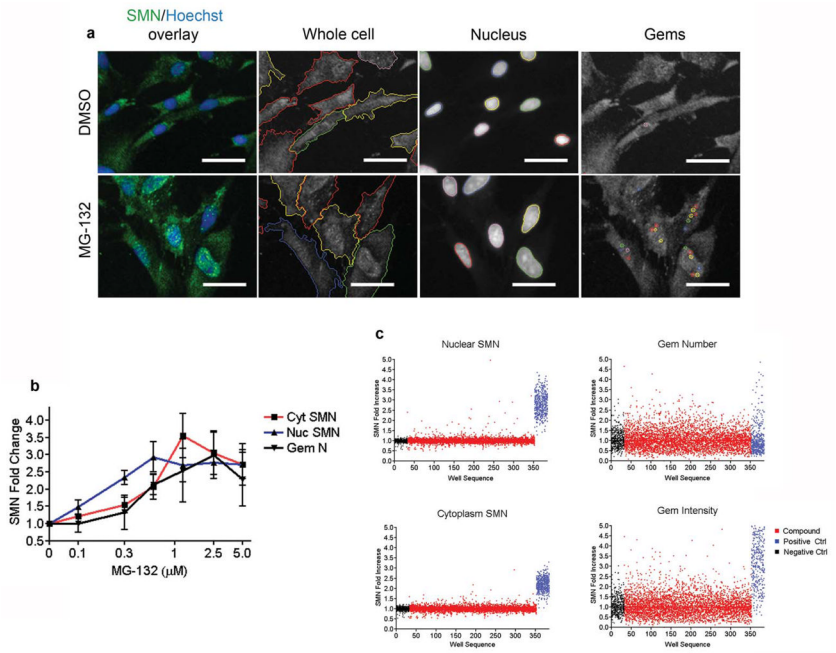

Figure 1. Development of a high content assay for SMN

(a) Representative images of cells treated with a control compound, MG-132 (1μM for 48 hours) or DMSO. Scale bars equal 20 μm. Cells were fixed and stained with an anti-SMN antibody and with Hoechst. Cytoplasmic and nuclear compartments and gems were defined as described in Supplementary Methods. (b) Dose response curves for increased SMN in different cellular compartments. Average values +/− s.d. are given. In this and all other figures, unless indicated, SMN values are normalized to those of DMSO-treated cells. (c) Scatter plots show the effects of representative sets of compounds from 15 separate screening plates on SMN levels in each compartment.

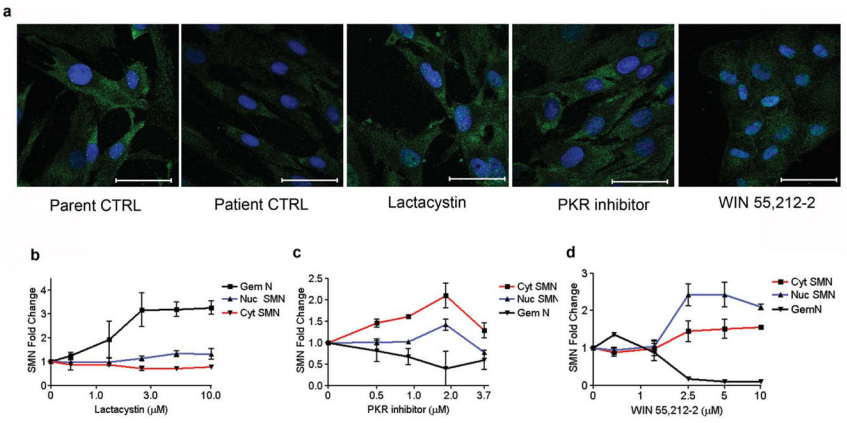

Figure 2. Identification of compounds that increase SMN in different intracellular compartments

(a) Representative images showing fibroblasts treated with lactacystin (2.5 μM), PKR inhibitor (1.8 μM) and WIN 55,212-2 (5 μM). Scale bars are 50 μm. Dose response curves showing examples of compounds that produce non-homogeneous increases in SMN in the different intracellular locations. (b) Lactacystin primarily increases gem numbers at 24 hours. (c) At certain concentrations, the oxindole-based PKR inhibitor preferentially increases cytoplasmic SMN at 72 hours. (d) WIN 55,212-2 up-regulates nuclear SMN more than cytoplasmic SMN at 72 hours. Error bars indicate +/− s.d.

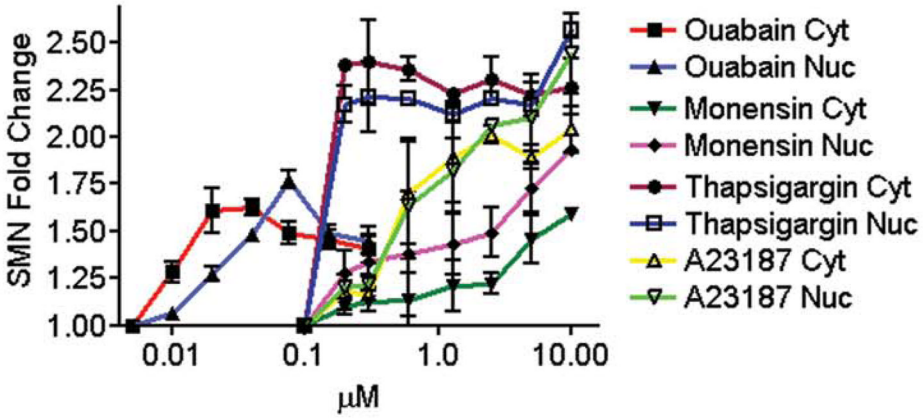

Figure 3. Compounds that elevate intracellular Na^+ or Ca^{2+} increase SMN levels

Dose response curves showing SMN increases produced by ouabain, monensin, A23187 and thapsigargin. Error bars indicate +/− s.d.

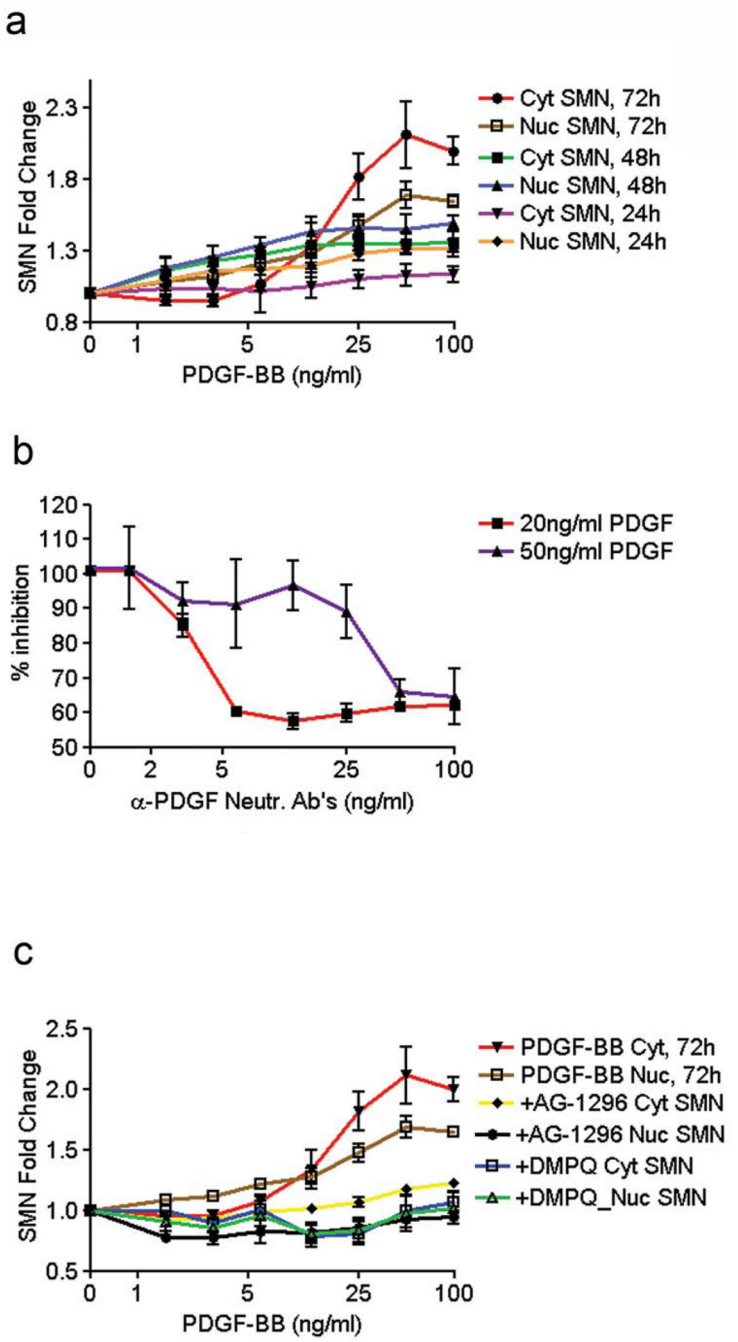

Figure 4. Growth factors increase SMN levels

(a) Dose response curves for 24, 48, and 72 hours of PDGF-BB treatment. (b) PDGF neutralizing antibodies block the increase in SMN produced by added PDGF (20ng/ml or 50ng/ml for 72 hours). (c) Pretreatment with 25 μM AG-1296 or DMPQ, small molecule inhibitors of the PDGFR kinase, block the ability of added PDGF to increase SMN. Data are presented as averages +/− s.d.

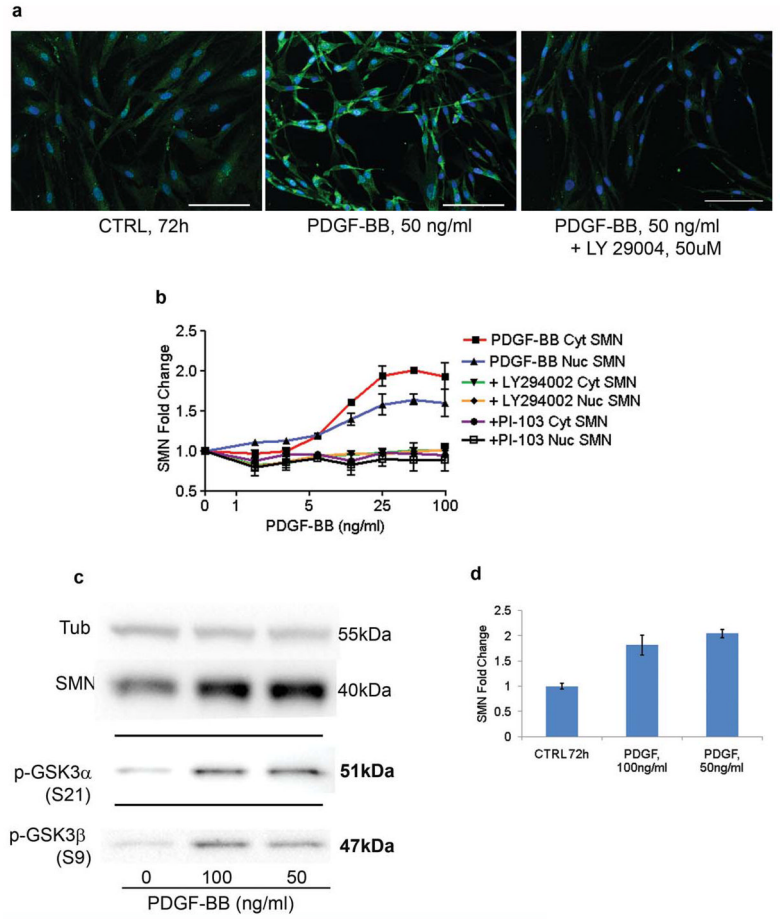

Figure 5. PDGF increases SMN through a signaling pathway involving PI3-K activation and GSK-3 inhibition

Fibroblasts were pre-incubated with individual inhibitors for 2 hours, and PDGF was then added. 72 hours later, plates were stained and imaged. (a) Micrographs of untreated fibroblasts and fibroblasts treated with PDGF alone or PDGF in the presence of the PI3K inhibitor, LY294002 (50 μM). Scale bar equals 50 μm. (b) Two different PI3K inhibitors, LY294002 (50 μM) and PI-103 (2 μM), were able to completely abolish the SMN increase induced by PDGF-BB. SMN fold increases are normalized to control wells that did not receive any inhibitor or PDGF. (c,d) Western blot quantification of SMN protein level shows that treatment with 50ng/ml PDGF-BB produces greater than a 2-fold increase of SMN after 72h treatment. Additionally, treatment with PDGF for 1h leads to inhibitory phosphorylation of GSK-3β on Ser9 and GSK3α on Ser21 detected by Western blot.

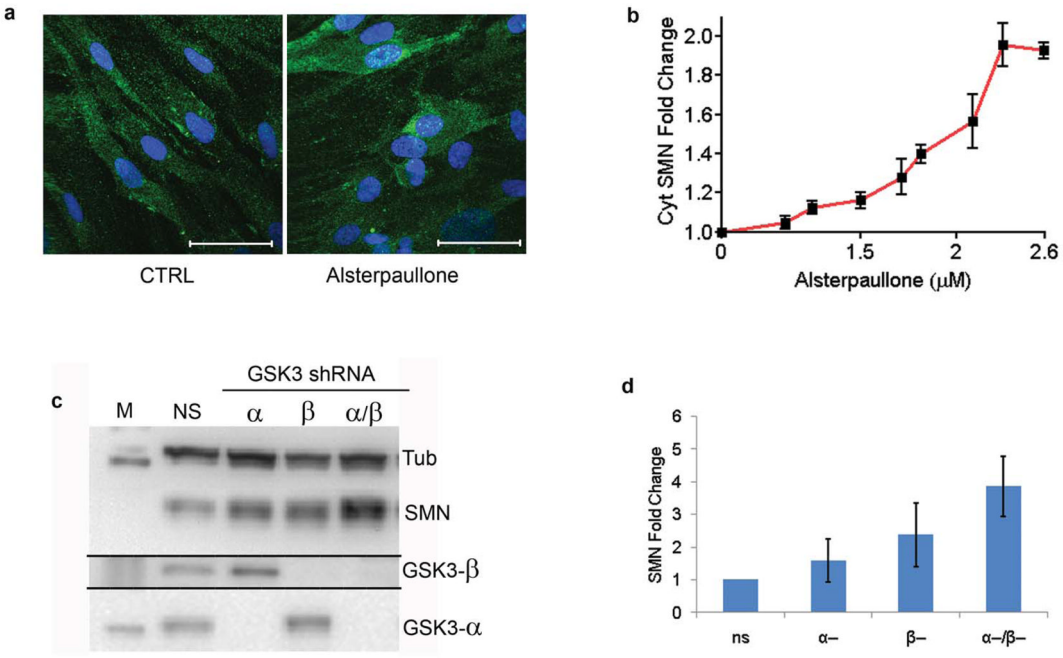

Figure 6. Inhibition of GSK-3 increases SMN

(a) Confocal images of patient fibroblasts treated with 1.5uM Alsterpaullone. Scale bars equal 50 μm. (b) Dose curve shows that alsterpaullone increases SMN in patient fibroblasts after 72 hour treatment. (c) Lentiviral delivery of shRNAs directed against GSK-3α or β decreases enzyme levels and increases SMN. (d) Data from 3 separate Western blots are averaged. SMN levels are normalized to tubulin and are seen to increase as much as 5-fold in individual experiments after reduction of both GSK-3 isoforms.

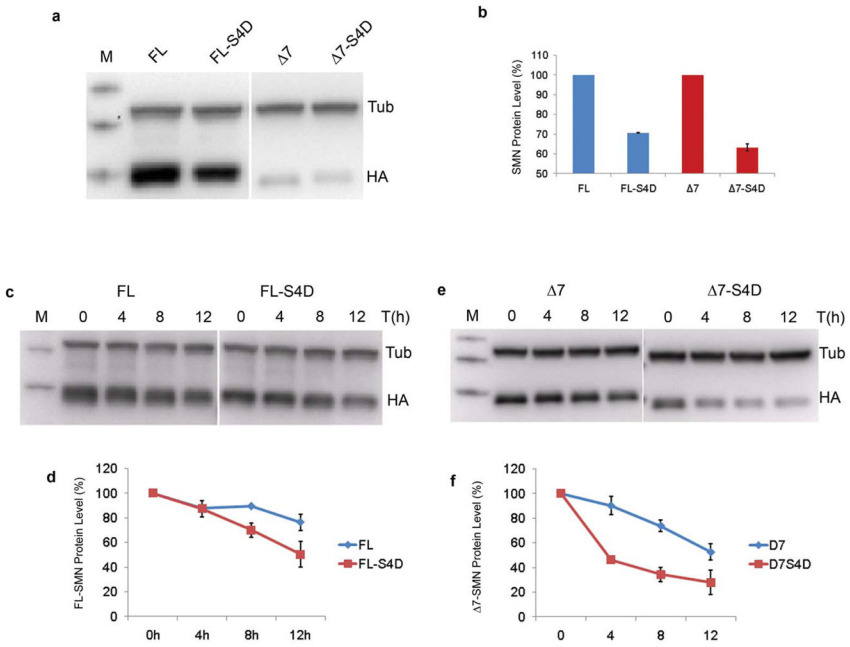

Figure 7. GSK-3 inhibition increases SMN levels by decreasing the rate of SMN degradation

(a,b) Levels of SMN in cells expressing wildtype or S4D mutants of full length or Δ7 forms of SMN. Lower levels are associated with expression of the mutant forms (which are normalized to their respective wildtype proteins). Levels of SMN in cells expressing the mutated forms of SMN are expressed as percent of their equivalent wildtype form. (c,d) Full-length SMN or the S4D mutants were expressed in HEK cells which were then treated with cycloheximide to block new protein synthesis. The S4D mutant form is degraded more rapidly over the next 12 hours. (e,f) Similar experiments done comparing wildtype and S4D mutants of the Δ7 form show an even bigger increase in the rate of degradation. Data are presented as averages of at least duplicate experiments +/− s.d.

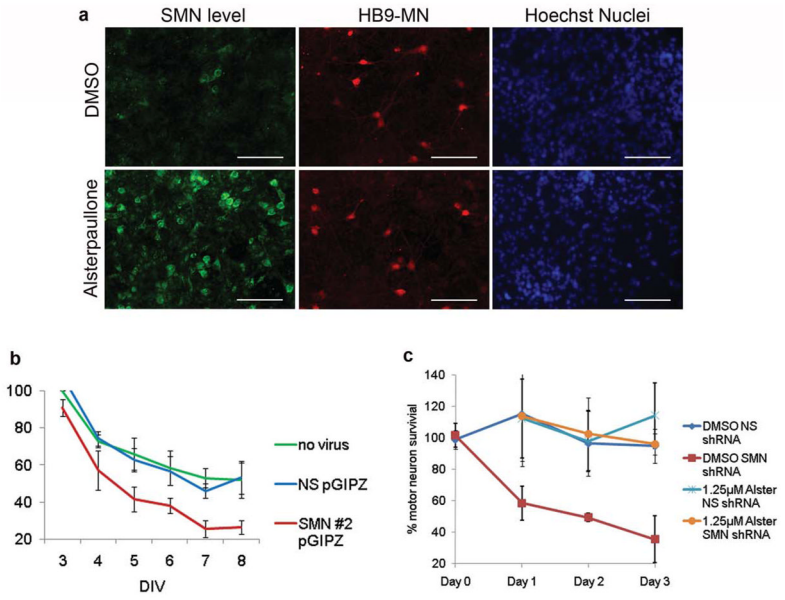

Figure 8. GSK-3 inhibitors increase SMN levels in mESC-derived motor neurons and prolong survival after shRNA knockdown of SMN

(a) Alsterpaullone increases SMN in mouse ES cell-derived motor neurons at 48h. Scale bars equal 50 μm. (b) Motor neuron survival assays were performed using control cells (no virus) or cells treated with non-silencing (NS) or SMN#2 pGIPZ lentivirus. The percentage of motor neuron survival was normalized to no virus control cells on Day 3. (c) Quantification of survival data for cells treated with 1.25 of alsterpaullone. Survival values are normalized to the survival levels of untreated motor neuron levels to focus on the death that was associated with reduction of Smn levels. Alsterpaullone had no effect on the motor neuron death that occurred in untreated cells maintained under normal culture conditions.